The biomagnetic signature of a crushed axon

A comparison of theory and experiment

J. M. van Egeraat,*‡ R. Stasaski,* J. P. Barach,* R. N. Friedman,* and J. P. Wikswo, Jr.*

*Living State Physics Group, Department of Physics and Astronomy, Vanderbilt University, Nashville, Tennessee 37235 USA; and
‡Department of Neurology, Faculty of Medicine, Erasmus University, 3000 DR Rotterdam, The Netherlands

ABSTRACT The response of a crayfish medial giant axon to a nerve crush is examined with a biomagnetic current probe. The experimental data is interpreted with a theoretical model that incorporates both radial and axial ionic transport and membrane kinetics similar to those in the Hodgkin/Huxley model. Our experiments show that the effects of the crush are manifested statically as an elevation of the resting potential and dynamically as a reduction in the amplitude of the action current and potential, and are observable up to 10 mm from the crush. In addition, the normally biphasic action current becomes monophasic near the crush. The model reflects these observations accurately, and based on the experimental data, it predicts that the crush seals with a time constant of 45 s. The injury current density entering the axon through the crush is calculated to be initially on the order of 0.1 mA/mm^2 and may last until the crush seals or until the concentration gradients between the intra- and extracellular spaces equilibrate.

INTRODUCTION

The sequence of physiological events following nerve injury is poorly understood, partially because of a lack of appropriate models and adequate measurement techniques. Although several reports on injured nerves can be found in the literature (2, 5, 6, 11, 21), none of them presents a model to explain the observed phenomena, possibly because the acquired data does not allow an in-depth, quantitative analysis. Most studies focus on the structural changes that can be visually detected (5, 6, 11), e.g., the formation of small vesicles or axosomes in the intracellular space after the injury. These vesicles are reported to migrate towards the injury site (5), supposedly for the purpose of reconstituting the membrane integrity (sealing). Yawo and Kuno (21) provide more quantitative data on the sealing process with microelectrode measurements of the impedance between the bath and the intracellular space of a transected cockroach giant axon. An inherent limitation of the use of microelectrodes is that data can only be obtained at a few selected positions along the axon, even though it may be desirable to characterize the nonuniform region close to the crush at more positions. In addition, the impalement and presence of multiple electrodes close to the injury site may affect the sealing process. Borgens (2) used a vibrating probe to measure the injury current entering a transected lamprey spinal cord. This technique allows the determination of slowly varying currents in the extracellular fluid surrounding the tissue; but, it has a limited spatial resolution so that an accurate determination of the current entering a single axon is not possible. Also, the temporal resolution is limited by the vibration frequency of the probe, usually ~400 Hz, which precludes detailed measurement of action signals propagating into the damaged region.

In this paper, we introduce the Biomagnetic Current Probe (17, 19) as a convenient method for the quantitative evaluation of nerve injuries. This device allows constant monitoring of the action current at many positions in the vicinity of the injury. Because direct physical contact between the probe and the tissue is not necessary, the sealing process is not affected by this technique. In an accompanying paper, van Egeraat and Wikswo (4) present a mathematical model to interpret the data acquired by applying the Biomagnetic Current Probe. This model can be used in cases where the intra- and extracellular ion concentrations are no longer constant as e.g. in the Hodgkin/Huxley model (10), but vary as a result of axial diffusion and membrane transport of ions. As demonstrated in (4), ionic diffusion may play an important role in nerve injury.

In order to illustrate the capabilities of the Biomagnetic Current Probe, we present a preliminary view of some of our data in Fig. 1. This magnetic scan consists of a sequence of measurements at different positions of the action current in a crushed crayfish medial giant axon. The data were obtained ~8 min after crushing. The action current far from the crush exhibits a biphasic pattern, which is normal for crayfish (1, 14). Close to the crush the amplitudes of both phases decrease, most notably for the (negative) second phase, so that the action current becomes relatively monophasic. These effects were accurately reproduced in all experiments. In this paper we will try to explain the data such as shown in Fig. 1, by performing simulation calculations with the diffusion model modified for the crayfish physiology.

METHODS

Experimental

Biomagnetic and bioelectric measurements were performed on the medial giant axons of 10 crayfish (*Procambarus Clarkii*). The crayfish

R. Stasaski's current address is Advanced Cardiovascular Systems, Inc., Santa Clara, CA 95052-8167, USA.

Address correspondence to Dr. John P. Wikswo, Jr., Living State Physics Group, Department of Physics and Astronomy, Vanderbilt University, P.O. Box 1807 Station B, Nashville, TN 37235.

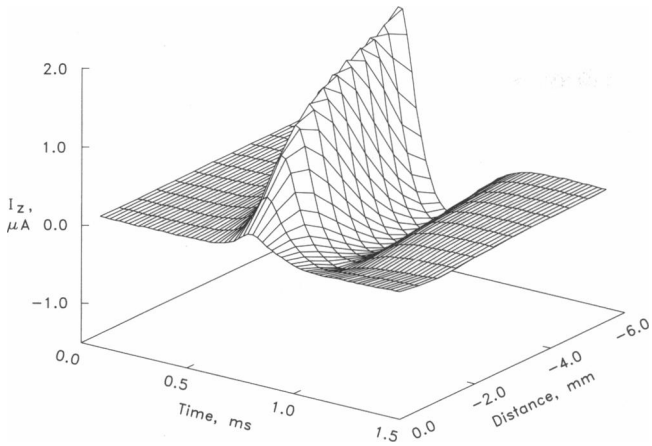

FIGURE 1 Time course of the measured action current, I_z, at 12 different axial positions along the medial giant axon of an isolated crayfish nerve bundle (0.5 mm spacing). The crush was at 0.0 mm. The data were taken ~8 min after crushing.

were dissected in Van Harreveld's solution (15), Tris buffered to a pH of 7.4 at 22°C. The appendages and exoskeleton were removed and the nerve bundle was cleared of muscle from the tail to the esophageal connectives. The ends of the nerve bundle were ligated and the cord was transferred to the recording chamber.

We stimulated one of the esophageal connectives extracellularly with a 4 Hz pulse (100 μs pulse width), just above the threshold amplitude. The response of the lateral axon could be separated from that of the medial axon because of the difference in arrival times at the recording site. Initially, recordings of bioelectric and biomagnetic signals were obtained from the undamaged preparation. Then, the nerve bundle was crushed with No. 5 forceps encased in plastic tubing (0.7 mm diameter) so as not to tear the axon or sheath. The position of the crush was always more than 20 mm from the stimulus site in order to allow the development of a uniformly propagating action signal.

Biomagnetic measurements involved threading the nerve bundle through a toroidal pick-up coil which consisted of a ferrite core, wound with 65 evenly spaced turns of 40 gauge (0.074 mm diameter) insulated copper wire (8). The ferrite core had a square cross section, with inner and outer radii of 1.05 and 1.95 mm, respectively, and a width of 1.25 mm. It was insulated from the bath by an epoxy coating, which changed the coil radii to 0.75 and 2.25 mm, respectively, and the width to 1.90 mm. The current induced in the toroid was detected by a room-temperature, low-noise amplifier (17). A frequency compensator was used to correct for the frequency response of the toroid and amplifier system (16). Since this biomagnetic measurement is easily performed and presents no stress to the axon, numerous measurements could be taken. Typically, recordings were taken with 0.5 mm increments in a region of 12–15 mm around the crush.

Bioelectric measurements were performed using a glass microelectrode filled with 3 M KCl and having an impedance of 40 MΩ, coupled to an electrometer (model M701; World Precision Instruments, Inc., New Haven, CT). Although multiple, simultaneous bioelectric and biomagnetic recordings were desired, we obtained complete scans of the crushed region of all axons with the magnetic method only. Multiple microelectrode recordings were obtained in only three experiments, but they were not sufficient in number and the time between impalements was too long to allow a detailed analysis of the spatial variations in the signals. However, some electric recordings were useful for the validation of our numerical model.

Both the bioelectric and biomagnetic signals were amplified, low pass filtered at 25 kHz and averaged (model 1170 Signal Averager; Nicolet Instrument Corp., Madison, WI). In the nonscanning, simultaneous magnetic/electric recordings before crushing we took 256 averages. In order to keep the scanning time as short as possible, the magnetic signals were averaged 64 times at each position during scans, taking 16 s per position at the given stimulus rate. After crushing, we needed 2 min for setup, after which a scan was begun at 6 mm distal from the crush. We checked that no action signals propagated into the distal segment by scanning the probe with 0.5 mm increments towards the crush, which was reached after 4 min of scanning time. The continued scan over a 6 mm region proximal to the crush took ~4 min as well, which means that this region was scanned between 6 and 10 min after crushing. After this initial magnetic scan we attempted to complement our measurements with electric recordings; but, as indicated before, we did not succeed in getting similarly detailed spatial information with this technique.

Analytical

Modifications were made to the mathematical model described in the accompanying paper (4) to account for the crayfish physiology. The modeled axon was divided into 120 elements of 0.25 mm length, submerged in a grounded, infinite bath having constant ionic concentrations. Following crush, each of the intracellular concentrations varies as a result of both axial diffusion, governed by the Nernst/Planck diffusion equation, and radial flux, described by membrane kinetics similar to the Hodgkin/Huxley model (10). The first element is stimulated with a pulse just greater than threshold.

The nerve crush is modeled as a nonspecific, ionic diffusion pathway of variable size between the 120th element and the bath. We have defined a parameter, the crush factor, to account for various degrees of injury. If an area equal to the cross-sectional area of the axon participates in the diffusion, the crush factor is equal to unity. A partial injury, or sealing, may be modeled by a reduced crush factor. Table 1 lists the parameters which were used in the crayfish giant axon computer model. The extracellular concentrations are as specified for Van Harreveld's solution (15). The diffusion coefficients for sodium, potassium and chloride are equal to those in water at 22°C (13). The remaining ion species are covered in three categories, anions (A^-), divalent cations (C^{2+}), and large macromolecules, i.e., proteins (M^-). For the anions and divalent cations, we took an average of the diffusion coefficients of the ions that constitute these two categories (HCO_3^-, Ca^{2+}, Mg^{2+}, etc.). The intracellular proteins (M^-) do not diffuse as a result of their strong surface binding in the intraaxonal space (7).

The intracellular sodium concentration and the maximum membrane conductivity for sodium are in the range found by Muramatsu et al. (12). The axoplasmic potassium concentration corresponds to an equilibrium potential for potassium that is 5 mV below the observed resting potential of −80 mV; and, the ratio of the maximum membrane conductivity for sodium and potassium is close to values found in the literature (1). As suggested by Young and Moore (22), we raised the Hodgkin/Huxley model parameter n to the third power in the calculation of the membrane potassium flux. The chloride equilibrium potential is equal to the resting potential with the given intracellular concentration. The chloride membrane conductivity is taken from steady-state cable model studies (9), since chloride's only significant contribution is to the resting membrane conductivity. The membrane can be modeled as impermeable for the other anions and cations and the proteins.

The remaining three parameters, the intracellular anion, cation and protein concentrations, were derived from the intracellular conductivity, σ_i, determined by a core conductor model (1, 3). We found σ_i to be equal to 1.2 S/m, well within the range found in the literature (1, 9, 14). However, the intracellular conductivity is also a function of the intracellular ion concentrations $[s]_i$ (valence z_s) and diffusion coefficients D_s, namely,

TABLE 1 Parameters for the simulation model of the crayfish medial axon

Ion	$[s]_i$	$[s]_e$	D_s	$g_{s,max}$
	mM	*mM*	10^{-9} m^2/s	S/m^2
Na^+	22	192	1.2	450
K^+	153	5	1.8	150
Cl^-	10	237	1.9	5
A^-	0	2	1.2	0
C^{2+}	0	21	1.5	0
M^-	165	0	0	0

$V_{rest} = -80$ mV
$C_{mem} = 6.0$ mF/m^2
Axon radius = 100 μm
Temperature = 22°C

$$\alpha_n = \frac{0.053(-V + 11.5)}{e^{(-V+11.5)/7} - 1}$$

$$\beta_n = 0.100e^{-(V-80)/30}$$

$$\alpha_m = \frac{6.64(-0.35V + 7.1)}{e^{-0.35V+7.1} - 1}$$

$$\beta_m = 33.2e^{-V/250}$$

$$\alpha_h = 0.232e^{-V/10}$$

$$\beta_h = \frac{6.64}{e^{-0.15V+5.5} + 1}$$

($V = V_{mem} - V_{rest}$ in mV, α's and β's in ms^{-1})

A^- and C^{2+} indicate anions and cations, respectively (excluding sodium, potassium and chloride). $[s]_i$ and $[s]_e$ are the intra- and extracellular ion concentrations of ion species s, respectively. D_s is the diffusion coefficient and $g_{s,max}$ the maximum membrane conductivity. The α's and β's are the rate constants as defined in Hodgkin and Huxley (10) adapted for the crayfish physiology.

$$\sigma_i = \frac{F^2}{RT} \sum_s z_s^2 D_s [s]_i$$

with

$$s = (Na^+, K^+, Cl^-, A^-, C^{2+}, M^-), \qquad (1)$$

where F is the Faraday constant, R the gas constant and T the absolute temperature (in our case 295 K). The protein term $[M^-]_i$ in this summation is negligible because D_M is small (7), and hence the equation can be solved for the combined anion and cation concentration (excluding Na^+, K^+, and Cl^-), which was found to be close to zero. The protein concentration in Table 1 thus follows from the electroneutrality condition. So far we have assumed that proteins are monovalent, but this is not important for our analysis. Multivalency would alter the protein concentration, but it would not affect the results because the diffusion coefficient is assumed to be small compared to other ions.

The potassium gate kinetics, expressed by α_n and β_n, were taken from the literature (22), and were adjusted for the experimental temperature with a q_{10} of $e = 2.72$. The sodium gate kinetics, listed in Table 1, are the result of a fit of the theoretical action current and potential corresponding to the experimental data, with the squid rate constants (10) as an initial trial.

The membrane capacitance is an established value for this preparation (1). The radius of the axon used for our calculations was 100 μm, as determined by light microscopy.

As a demonstration of the merits of the model, Fig. 2 shows the match of our simulation results to the recorded data from the undamaged axon (crush factor equal to zero). In Fig. 2 *a*, we see the closeness of fit of the simulated action potential to the experimentally-recorded wave form. A comparison of the recorded and simulated action currents (Fig. 2 *b*) demonstrates that the computer model successfully describes the recorded behavior. The simulated action current is spatially averaged over five elements, corresponding to the width of the toroid that was used to obtain the experimentally-recorded action current. The discrepancy in the amplitudes of the positive phases may be attributed to a slightly incorrect high-frequency compensation of the amplifier or to geometric factors (14), since these most-strongly affect the sharp peaks in the action signals. The measured conduction velocity of 15.0 m/s matched closely with 15.6 m/s value determined by the model.

RESULTS

Our model predicts that, with a crush factor equal to one, the axial ionic current in the axon at the crush equals -3.38 μA (i.e., the current enters the axon) in the first seconds after crushing. This current is composed of the following ionic fluxes: sodium (-4.90 μA), potassium ($+1.31$ μA), chloride ($+2.06$ μA), other anions (0.02 μA) and divalent cations (-1.87 μA). The injury current is maximal at the crush and decreases quickly with distance to an almost negligible value 10 mm from the crush. This distance is comparable to the length constant of the axon, which is ~6 mm with the model parameters that we used. The injury current also decreases with time as more and more of the axon becomes permanently depolarized. The maximum current density at the crush, obtained by dividing the current by the axon cross-sectional area, is -0.11 mA/mm^2. As demonstrated for a squid giant axon in the accompanying paper (4), this large current may flow for prolonged periods of time, without great changes in the membrane potential, due to concentration differences and the associated ion fluxes across the membrane separating the intra- and extracellular spaces. The current that enters through the crush is mostly carried by sodium; but, most of the charge entering the axon leaves again as a potassium current through the membrane in the vicinity of the crush, limiting the voltage change on the membrane. Although it may take very little net charge to depolarize the membrane of an axon, it takes considerably more charge transport to equilibrate the concentrations.

In our experiments, we observed that the axon could survive for hours after crushing. However, the simplest model would predict that after such a long period of time, the intracellular space of the crushed axon would have an ionic composition identical to that of the extracellular medium; so, the entire axon would cease to function. Metabolic pump mechanisms such as the Na/K pump are not sufficiently powerful to compensate for the ion exchange at the crush (4). Therefore, the model had to be extended to include sealing of the crushed membrane. We assumed that the seal reduced the diffu-

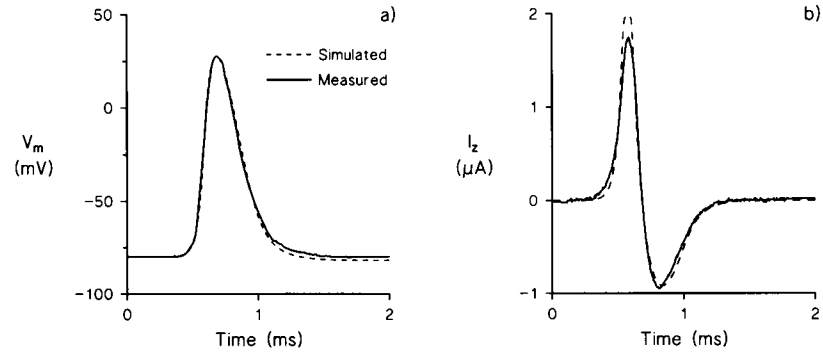

FIGURE 2 Comparison of an intracellularly-recorded and a simulated action potential (*a*) and the magnetically-recorded and simulated action current (*b*) of a normal crayfish medial giant axon.

sion between the intra- and extracellular spaces (i.e., reduced the crush factor), and also that the seal separated the distal part of the axon from the proximal by forming a partition-like structure at the site of the crush in the intracellular space. This is in accordance with observations by Yawo and Kuno (21). The time dependence of the crush factor $CF(t)$ was modeled as an exponential relation

$$CF(t) = CF(0)e^{-t/\tau_{seal}}, \tag{2}$$

in which τ_{seal} is the time constant of sealing. We evaluated the model for several values of τ_{seal}. Eq. 2 can be justified by the observation of Yawo and Kuno (21) that the sealing time depends on the availability of calcium in the extracellular space. After crushing, the calcium current I_{Ca} entering the axon depends on the crush factor; but, the decrease of the crush factor with time, in turn, depends on the calcium influx, or

$$I_{Ca} \propto CF \propto -\frac{dCF}{dt}, \tag{3}$$

which after integration leads to the exponential relationship expressed in Eq. 2. Eq. 3 is only a first order approximation, because the calcium influx also depends on the Ca^{2+} concentration gradient and the voltage gradient at the crush, according to the Nernst/Planck diffusion equation. However, in the results we present here, the most important factor affecting the calcium influx is the

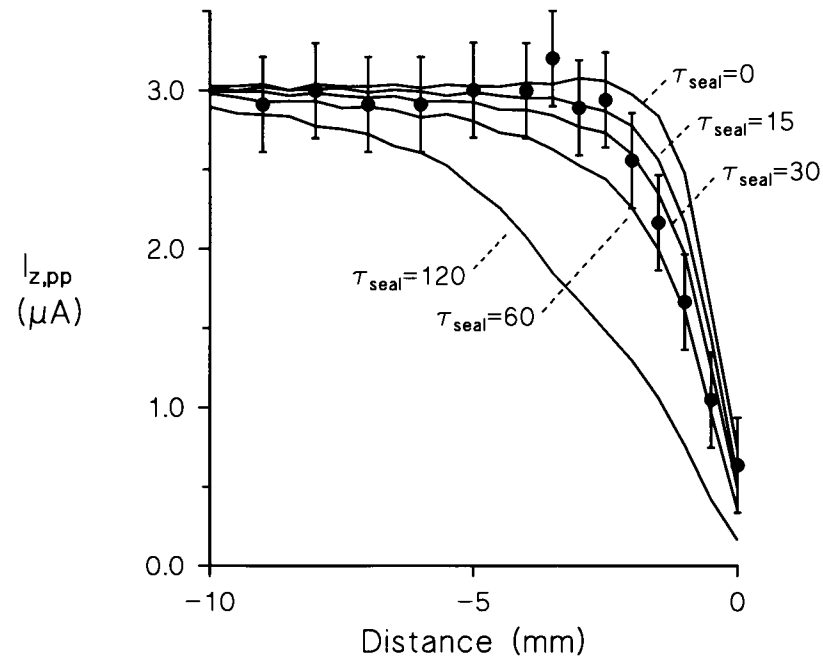

FIGURE 3 Comparison of the experimental (*circles* with *error bars*) and simulated (*solid lines*) peak-to-peak amplitudes of the action current in a crushed crayfish medial giant axon as a function of the distance from the crush. The times indicated are the assumed sealing time constants, τ_{seal}, in seconds. The error bars give the estimated measurement error in the amplitude according to (14).

crush factor. A more extensive model could explicitly include the calcium flux and a hypothetical mechanism by which calcium mediates in the sealing process.

The injury current cannot be detected with our inductively coupled current probe, because this current varies too slowly. Therefore, when an action signal is propagating towards the crush, the toroid will only measure the action current, which is superimposed on the nearly steady injury current. The recorded action current at several axial positions relative to the crush was shown in Fig. 1. We used our model to calculate the equivalent action current behavior. Fig. 3 gives a comparison of the experimental and simulated peak-to-peak amplitudes of the action current as a function of the distance from the crush for sealing time constants, τ_{seal}, up to 2 min. In all our models, we assumed that the initial crush factor $CF(0)$ was equal to unity. The model predictions of the amplitude were calculated 8 min after the simulated time of crushing, approximately corresponding to the time that the first scan reached this nerve segment. The experimental data fits the simulated data best for a sealing time constant between 30 and 60 s, which means that the sealing became effective before the magnetic data were taken. Additional measurements revealed that the amplitude profile such as in Fig. 3 did not collapse as was found in calculations for a nonsealing squid giant axon given in the accompanying paper (4).

Fig. 4 *a* is the model equivalent of Fig. 1, calculated for a sealing time constant of 45 s. Fig. 4 *b* shows the difference between the experimental and the simulated data, which is on the same order of magnitude as the difference in Fig. 2 *b* (10% of the peak-to-peak amplitude). This suggests that the quality of the crush simulation is mainly limited by the general ability of the model to reflect the crayfish physiology.

Fig. 5 shows the predicted intracellular ion concentrations as a function of the distance from the crush 8 min after crushing. The composition of the axoplasm approaches the extracellular composition over a distance of a few millimeters from the crush. Sodium and potassium show the steepest changes. The low membrane conductivity for chloride prevents a rapid radial influx.

Fig. 6 shows the computed injury current as a function of time for several axial positions. The crush gives rise to a steady current which has an amplitude on the same order as the action current and is sustained over a period of several minutes. As sealing proceeds, the injury current decreases and eventually, the axial current close to the crush becomes smaller than the current somewhat further from the crush (see inset in Fig. 6). This is due to the intracellular concentration profiles that were built up in the first minutes after crushing, and now relax back to reestablish homogeneous intracellular concentrations. The injury current density of -0.11 mA/mm^2 is consistent with vibrating probe measurements of the current density spatially averaged over a cut lamprey spinal cord

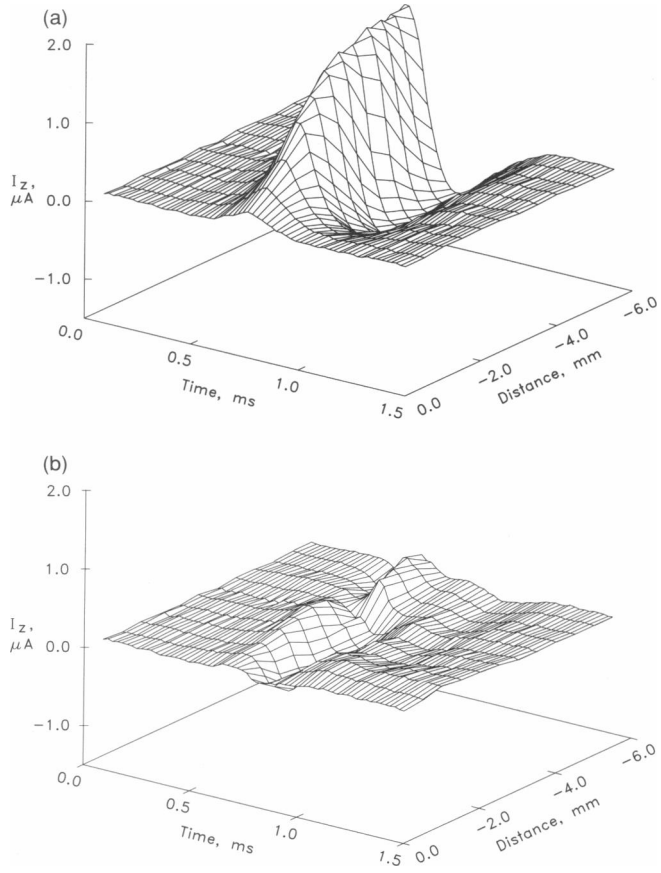

FIGURE 4 (*a*) Numerical simulation of Figure 1 with a sealing time constant, τ_{seal}, equal to 45 s. (*b*) Difference between Figs. 1 and 4 *a*. The standard deviation of the 768 data points with respect to $I_z = 0$ is 0.08 μA. The standard deviation from zero of the data in Figs. 1 and 4 *a* is ~0.49 μA.

(2), which was found to be well over -0.01 mA/mm^2 shortly after transection.

The simulation results (Figs. 4, 5, and 6) were calculated at exactly 8 min after crushing. The experimental data, however, were taken in the time period from 6 to 10 min after crushing, which introduces an error caused by the nonsteady-state conditions. At this time, however, the crush is almost completely sealed and the intracellular concentrations are changing much slower than they did immediately after crushing, when steep concentration and voltage gradients exist. The maximum rate of change of the intracellular concentrations at this time was calculated to be less than 3% per minute so that the error introduced by the nonsteady-state conditions is small.

DISCUSSION

The magnetic measurement technique allows a detailed study of nonuniform propagation in nerve fibers. The measured and predicted biomagnetic signatures of a crushed crayfish medial axon (Figs. 1 and 4) show excel-

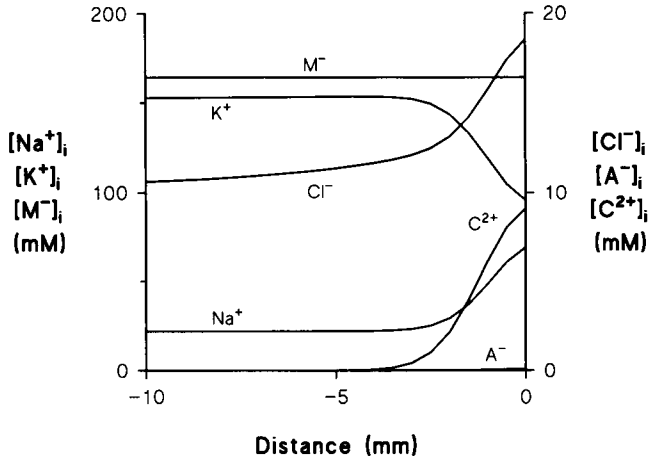

FIGURE 5 The simulated intracellular concentrations of the different ion species as a function of the distance from the crush, after 8 min of simulation time following the simulated crush. The assumed sealing time constant, τ_{seal}, was 45 s.

lent agreement. These studies confirm that the crush acts as a diffusion path to the bath which causes ionic current to flow at the site of injury. These injury currents may be accurately modeled by the Nernst/Planck equation and, close to the crush, the current density can be on the order of 0.1 mA/mm^2. We could not detect these currents with our present recording technique, which is based on inductive pick-up; but, newly developed SQUID magnetometers should allow a direct measurement (18, 20).

The ionic currents change the intracellular ion concentrations, which in turn modify the equilibrium potentials for the various ion species. As a result, action signals approaching the crush will change in amplitude and shape and, ultimately, the propagation will fail. The principle of self-similar propagation that is used in studies of undamaged axons (14) is not valid in this case. In particular, the action currents tend to change from a normal biphasic signal into a monophasic signal before they disappear.

Nerve sealing following injury, necessary to preserve nerve function, occurs with a time dependence that can be examined using our model. In our calculations, we assumed an exponential decrease of the crush size with time. The modeled sealing process could be made dependent on the diffusion of calcium or other agents that affect sealing. Future studies will address this. A microelectrode study of transected nerve fibers of the cockroach (21) indicates that sealing occurred within 5 to 30 min after transection. Our analysis for crush injuries in crayfish gives shorter sealing times, possibly due to the differences in species and type of injury.

We presented experimental data that were taken no sooner than ~8 min after crushing. Taking into account the time necessary to complete a magnetic scan in a region of 6 mm proximal to the crush (4 min) and the relatively fast changing state of the nerve in the first minutes after crushing (see, e.g., Fig. 6), this is probably a good time to perform the scan. The finite scan time would not allow an accurate picture of the momentary spatial variations in amplitude during the first minutes after crushing because the nerve has not yet reached a state that can be called steady on the time scale of the scan time. On the other hand, measurements long after the nerve has sealed may be expected to give roughly similar results for all nerves because the intracellular concentrations have equilibrated over the entire intracellular space of the axon. The numerical analysis was performed for the experimental data from one experiment, but in all experiments we found qualitatively similar results, i.e., all axons sealed and did not show a collapse of the action current amplitude profiles. In future experiments it may be possible to decrease the scan time by measuring simultaneously at many positions with multiple magnetic probes. This would allow inspection of the events shortly after crushing and increase the accu-

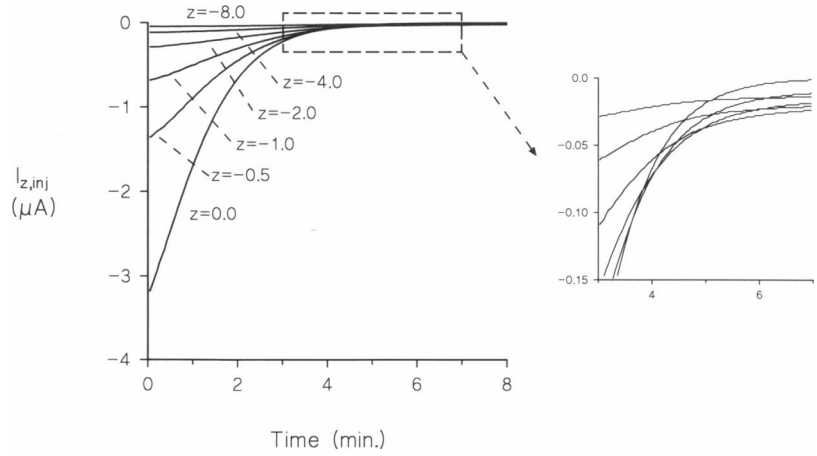

FIGURE 6 The time course of the axial injury current, $I_{z,inj}$, at different axial positions z. (*Inset*) Note that the order of the magnitude of the individual currents changes approximately 4 min after crushing. The assumed sealing time constant, τ_{seal}, was equal to 45 s in this simulation.

racy of the sealing time constant or even lead to improvements to our exponential model of sealing.

The presence of the toroid may seem a complicating, distorting factor in the extracellular space. However, Roth and Wikswo (14) showed that the toroid has negligible effect on the volume conduction currents and measured signals when it is small compared to the spatial extent of the action potential, which was the case in our experiments. On the other hand, the clearance between the nerve cord and the toroid was sufficiently large that axial diffusion in the extracellular space along the axon was not hampered: the clearance cross-sectional area was approximately ten times the axonal cross-sectional area.

When studying injury of nerve bundles, the magnetic technique may prove especially useful, because the signal amplitude is more accurately related to the number of active axons in the bundle than is the case for extracellularly recorded electric signals, which are very sensitive to extracellular conductivity and geometry (19). In clinical applications one could use an openable toroidal sensor that can be clipped around the nerve bundle (8). Although myelinated, mammalian nerves are quite different from a crayfish giant axon, the study of injured nerves at the cellular level is a first step towards the understanding of injury in more complex systems.

This study demonstrates that the ability to scan the toroidal pick-up coil of the Biomagnetic Current Probe along an axon and thereby measure the axial variation of intracellular action currents offers significant advantages over multiple microelectrode penetrations. Other measurements that might benefit from this approach include studies of the squid giant synapse, axonal transport, and non-uniform propagation at axonal bifurcations.

This grant was supported in part by NIH grant NS19794.

Received for publication 18 July 1991and in final form 1 November 1992.

REFERENCES

1. Barach, J. P., B. J. Roth, and J. P. Wikswo, Jr. 1985. Magnetic measurement of action currents in a single nerve axon: A core conductor model. *IEEE Trans. Biomed. Eng.* BME-32:136–140.
2. Borgens, R. B. 1988. Voltage gradients and ionic currents in injured and regenerating axons. *In* Advances in Neurology: Functional recovery in neurological disease. S. G. Waxman, editor. Raven Press, New York. 51–66.
3. van Egeraat, J. M., R. N. Friedman, and J. P. Wikswo, Jr. 1990. The magnetic field of a single muscle fiber: First measurements and a core conductor model. *Biophys. J.* 57:663–667.
4. van Egeraat, J. M., and J. P. Wikswo, Jr. 1993. A model for axonal propagation incorporating both radial and axial ionic transport. *Biophys. J.* 64:1299–1305.
5. Fishman, H. M., K. P. Tewari, and P. G. Stein. 1990. Injury-induced vesiculation and membrane redistribution in squid giant axon. *Biochim. Biophys. Acta.* 1023:421–435.
6. Gallant, P. 1988. Effects of the external ions and metabolic poisoning on the constriction of the squid giant axon after axotomy. *J. Neurosci.* 8:1479–1484.
7. Gershon, N. D., K. R. Porter, and B. L. Trus. 1985. The cytoplasmic matrix: its volume and surface area and the diffusion of molecules through it. *Proc. Natl. Acad. Sci. USA.* 82:5030–5034.
8. Gielen, F. L. H., B. J. Roth, and J. P. Wikswo, Jr. 1986. Capabilities of a toroid-amplifier system for magnetic measurement of current in biological tissue. *IEEE Trans. Biomed. Eng.* BME-33:910–921.
9. Glantz, R. M., and T. Viancour. 1983. Integrative properties of crayfish medial giant neuron: steady-state model. *J. Neurophysiol.* 50:1122–1142.
10. Hodgkin, A., and A. F. Huxley. 1952. A quantitative description of membrane current and its application to conduction and excitation in nerve. *J. Physiol. (Lond.).* 117:500–544.
11. Meiri, H., A. Dormann, and M. E. Spira. 1983. Comparison of ultrastructural changes in proximal and distal segments of transected giant fibers of the cockroach *Periplaneta americana. Brain Res.* 263:1–14.
12. Muramatsu, I., M. Fujiwara, A. Miura, and T. Narahashi. 1985. Effects of goniopora toxin on crayfish giant axons. *J. Pharmacol. Exp. Ther.* 234:307–315.
13. Robinson, R. A., and R. H. Stokes. 1959. Electrolyte Solutions. Butterworth, London. 560 pp.
14. Roth, B. J., and J. P. Wikswo, Jr. 1985. The magnetic field of a single nerve axon. A comparison of theory and experiment. *Biophys. J.* 48:93–109.
15. Van Harreveld, A. 1936. A physiological solution for freshwater crustaceans. *Proc. Soc. Exp. Biol. Med.* 34:428–432.
16. Wikswo, J. P., Jr., P. C. Samson, and R. P. Giffard. 1983. A low-noise, low input impedance amplifier for magnetic measurements of nerve action currents. *IEEE Trans. Biomed. Eng.* BME-30:215–221.
17. Wikswo, J. P., Jr. 1985. Current probe system for measuring cellular action currents. *In* Biomagnetism: Applications and Theory. H. Weinberg, G. Stroink, and K. Katila, editors. Pergamon Press, New York. 83–87.
18. Wikswo, J. P., Jr., R. N. Friedman, A. W. Kilroy, J. M. van Egeraat, and D. S. Buchanan. 1990. Preliminary measurements with microSQUID. *In* Advances in Biomagnetism. S. J. Williamson, M. Hoke, G. Stroink, and M. Kotani, editors. Plenum, New York. 681–684.
19. Wikswo, J. P., Jr., and J. M. van Egeraat. 1991. Cellular magnetic fields: fundamental and applied measurements on nerve axons, peripheral nerve bundles, and skeletal muscle. *J. Clin. Neurophysiol.* 8:170–188.
20. Wikswo, J. P., Jr., J. M. van Egeraat, Y. P. Ma, N. G. Sepulveda, D. J. Staton, S. Tan, and R. S. Wijesinghe. 1990. Instrumentation and techniques for high-resolution magnetic imaging. *In* Digital Image Synthesis and Inverse Optics. A. F. Gmitro, P. S. Idell, and I. J. LaHaie, editors. *SPIE Proceedings.* 1351:438–470.
21. Yawo, H., and M. Kuno. 1985. Calcium dependence of membrane sealing at the cut end of the cockroach giant axon. *J. Neurosci.* 5:1626–1632.
22. Young, S. H., and J. W. Moore. 1981. Potassium ion currents in the crayfish giant axon. *Biophys. J.* 36:723–733.